

EPIC IN ORBIT BACKGROUND

D.H. Lumb¹

ESA Payload Technology Division, Research and Scientific Support Department, ESTEC, Postbus 299, NL-2200 AG Noordwijk, The Netherlands

ABSTRACT

We briefly describe the methods used in compiling a set of high galactic latitude background data. The characteristics and limitations of the data which affect their use as a template for analysing extended objects are described. We briefly describe a spectral fitting analysis of the data which reveals a normalisation for the extragalactic background of $11.4 \text{ keV cm}^{-2} \text{ s}^{-1} \text{ sr}^{-1}$, which implies the fraction of hard X-ray background presently resolved by various Chandra observations is towards the lower limit of their estimates.

Key words: Missions: XMM-Newton

1. INTRODUCTION

Many users have asked for background data sets with which to analyse extended objects, particularly where determination of background is difficult from their own data sets. We have developed some event lists for each EPIC camera that could be used *ad interim*. These files have an extension containing a calibrated event list in the same format as produced by SAS. Compared with previous efforts, the new sets (ca. December 2001) are significantly longer to allow improved signal:noise (typically the exposure duration is about an order of magnitude longer than the normal GO data set); the data are homogeneously collected from high galactic fields with no bright sources; the data set uses homogeneously the THIN filter only and EXPOSURE,STDGTI, BADPIX and EVENTS extensions of the files have all been concatenated and made coherent, so that in principle the observer could use them as a coherent data set for extractions via various *SAS* or *ftool* procedures, without making the manual corrections and calculations that were required for the previous incarnation.

Many diverse aspects of the XMM-Newton radiation environment were discussed extensively at a Workshop held in December 2000. The reader is invited to look at the links under /docs/documents/ pages of the VILSPA web site, particularly the document: CAL-MIN-0002-0-0.html. This has pointers to viewgraphs and minutes from the Workshop. The present note concerns *quiescent* back-

ground (i.e. after removal of proton flares via. GTI filtering).

2. DATA SELECTION

2.1. FIELD LOCATIONS

We have had to resort to compiling data from blank sky fields. To do so with realistic S:N ratios for each of 4 instrument modes would impose an unacceptable penalty on Guest Observer science programme time, so we concentrated on the Full Frame imaging modes which are generally used for the faint extended objects. To minimise statistical uncertainties, the effective exposure duration in our data sets should be an order of magnitude longer than that of the typical Guest Observer exposure. Again it was an unrealistic proposition to observe with the 3 EPIC optical blocking filters for ~ 300 ks each, specifically to obtain this required data, therefore we decided to make use of a variety of Guaranteed and Calibration Time observations of “blank” fields to compile our data serendipitously.

Suitable fields were almost all taken with the filter in THIN position, although this imposes additional complications for those users who might need to use a thicker optical blocking filter. Nevertheless as the soft diffuse X-ray component is more spatially and spectrally variable than the harder X-ray emission components this was not the major driver for our analysis.

Table 1 summarises the location of the fields selected.

2.2. DATA GENERATION

The data sets were processed using the pipeline processing of XMM-Newton Science Analysis Subsystem 5.2, in order to generate calibrated event lists for each EPIC camera. Proton flare GTI filtering was made on time bins of ~ 100 s at count rates ≥ 45 (20) events/bin in PN (MOS). Next we removed the signature of bright field sources by forming images in the 0.5 - 2keV band and running SAS task *EBOXDETECT*. Approximately 10 objects per field were identified and an exclusion of 25 arcsec radius applied around the detected centroids. This exclusion cannot be directly associated with a source flux level, but individual analysis of the fields confirmed the estimates based on LogN-LogS curves (Hasinger et al 2001), that sources of flux brighter than about $1 - 2 \times 10^{-14} \text{ ergs cm}^{-2}$

Table 1. Summary of target locations compiled

RA	Dec	Date of observation	Duration (ks)	N_H (10^{20} cm^{-2})	L II	B II
02:18:00	-05:00:00	2000-07-31	60	2.5	169.7	-59.8
02:19:36	-05:00:00	2000-08-04	60	2.55	170.35	-59.5
02:25:20	-05:10:00	2001-07-03	25	2.7	172.3	-58.6
02:28:00	-05:10:00	2001-07-06	25	2.7	173.5	-58.2
10:52:44	+57:28:59	2000-04-29	70	0.56	149.3	53.1
12:36:57	+62:13:30	2001-06-01	90	1.5	125.9	54.8
13:34:37	+37:54:44	2001-06-23	80	0.83	85.6	75.9
22:15:31	-17:44:05	2000-11-18	55	2.3	39.3	-52.9

s^{-1} (0.5-2 keV) have had about 80% of their flux removed with this recipe. Finally the screened data were co-added, and the exposure and GTI extensions of the FITS data files carefully added and concatenated together.

3. DATA CHARACTERISTICS

3.1. FLUORESCENT EMISSION LINES

The passage of charged particles through the cameras is associated with generation of fluorescent X-ray emission. This emission is most clearly seen in the form of emission line energies characteristic of the camera body materials (aluminium and stainless steel components for example). The construction of the two EPIC camera types is quite different, leading to substantially different manifestations of these features. The outer 6 of 7 CCDs detect more Al K radiation due to their closer proximity to the aluminium camera housing. Si K emission however is concentrated along the edges of some CCDs. In contrast the PN camera has a relatively intense contribution from energies around the Cu K line. What is notable is that this emission is spatially variable (Freyberg 2002).

The consequences for ignoring the spatial variation of these background features could be dramatic. XMM-Newton is possibly the observatory of choice for spectrally-resolved imaging of large clusters, for example to map radial temperature and element distributions. However the variable Al and Si background lines would compromise abundance determinations of cluster emission lines with moderate redshifts, while the variable high energy background would bias temperature measurements at large radii. These difficulties should be alleviated if the proposed background templates prove to be representative.

3.2. UNREJECTED PARTICLE BACKGROUND

A background component that is relatively constant in spectrum and with position, is the remnant events generated by charged particles which are not rejected by on-board or ground processing. Compared with a maximum predicted primary cosmic ray particle rate of $4 \text{ cm}^{-2} \text{ s}^{-1}$,

the measured rates in all the CCD cameras on XMM-Newton since launch have lain in the range 2 - $2.5 \text{ cm}^{-2} \text{ s}^{-1}$. The internal spectrum in the MOS1 camera, below 10keV, after selection for X-ray event characteristics (the SAS attributes *(#XMMEA_EM && PATTERN in [0:12])*) is $0.026 \text{ events cm}^{-2} \text{ s}^{-1}$. Of this $0.021 (\pm 0.0022) \text{ cm}^{-2} \text{ s}^{-1}$ is in the flat spectrum component, the remainder in emission line components and noise component increasing to lower energies. The flat spectrum count rate implies a cosmic ray rejection efficiency of $\sim 99\%$ as expected. The equivalent spectrum in the PN cameras after applying the SAS attributes *#XMMEA_EP && PATTERN in [0:4]* is $0.039 \text{ cm}^{-2} \text{ s}^{-1}$ is in the flat spectrum component, and $0.034 \text{ cm}^{-2} \text{ s}^{-1}$ in the fluorescent lines. This could imply a reduced rejection efficiency than MOS or a higher detection efficiency to local γ 's as a consequence of the much thicker pn detection thickness.

3.3. LOW ENERGY ARTEFACTS

The most obvious features in the lowest energy band are effects of "bad pixels". A pixel which is consistently bad is flagged for removal on-board by loading a table of positions to be blanked out. Some pixels "flicker" on and off (Hopkinson 1992) with low recurrence rate ($\leq 1\%$), and the efficiency for finding them post-facto in the SAS pipeline is dependent on many factors, so that some such events may occur in the background template and not the observer's data set and vice versa.

In the PN camera there are occasional blocks of bright pixels, typically 4 pixels in height. Their presence varies from observation to observation. They arise from an artefact of the CCD offset bias level calculation at the start of each observation.

4. SPECTRAL ANALYSIS

4.1. INTERNAL BACKGROUND

In principle one can use data from outside the filter rim as a measure of the true internal background. However as noted, this is not strictly true due to the spatial varia-

tion in fluorescent emission. This was easiest to perform in MOS, and therefore we modeled the internal background, with multiple Gaussian functions to characterise these emission lines, imposed upon a broken power-law to describe the continuum due to unrejected particle backgrounds, and low energy noise. In Fig 1 we show the comparison of this internal background component with the total spectrum including the CXB. The internal component should be scaled with its particle continuum according to the ratio of in- and out-of-field detector areas, but the emission line intensities must be allowed to vary (in order to account for the aforementioned spatial variation).

At energies ≤ 5 keV the CXB dominates, with a clear signature of low energy emission lines at $E \leq 1$ keV not present in the internal background, but most likely from a thermal cosmic plasma spectrum.

4.2. COSMIC X-RAY BACKGROUND

In the case of the MOS data files, where we are more secure of a subtraction of the internal background component, we attempted a simple spectral fit to the diffuse background spectrum. We adopted an empirical two temperature MEKAL (Mewe et al Mewe 1985) plus power-law component to describe the cosmic diffuse X-ray background. The former represent the contribution from the supposed Galactic Halo, and the latter the extragalactic unresolved AGN population. Temperatures of ~ 0.08 keV and ~ 0.21 keV together with a power law 1.4 could be recovered. We made an estimate of the sub-keV emission in some of the different fields noting differences in the measured temperature and flux. This variability in emission and lack of detailed temperature measurement capability hampers a more accurate determination of Galactic background properties. For example the measured mean deviation from field to field of 2 - 10 keV flux is about 3.5%, consistent with a uniform diffuse extragalactic background. On the other hand the mean deviation of 0.2 - 1 keV flux is about 35% from field to field.

The recovered spectral fitting parameters are consistent with a number of investigations of the diffuse X-ray background, which leads us to believe that the user should be able to use the sets with suitable caveats to analyse more general conditions with different filters and Galactic latitude, as described below. The calculated normalisation of extragalactic background was $11.4 \text{ keV cm}^{-2} \text{ s}^{-1} \text{ keV}^{-1} \text{ sr}^{-1}$, which is comparable with determination by SAX, but places the fraction of Chandra-resolved harder X-ray background towards the lower limits of claimed fractions (70% rather 95%).

5. CAVEATS FOR USE

The EPIC cameras allow a choice of optical blocking filter to prevent contamination by optically bright targets. For most extended and/or faint extragalactic targets, such

contamination is negligible, and the thinnest filter can be employed, as indeed was the case for all the observations compiled in this work. However should the observer have chosen a thicker filter, the transmission of diffuse background X-rays (and no doubt any remnant proton flux) will be reduced. Therefore the observer would have to model the differences in soft component based on the response matrices and limited knowledge of the expected Galactic emission.

The observer must take care to extract background from an appropriate location in the field of view. Most simply the extraction region should be defined in detector co-ordinates to match closely the region of the desired science target. In some applications the user would subtract data in sky co-ordinates. In this case the template event lists could be recast to mimic the nominal pointing direction of the observer's field (for example using SAS task *ATTCALC* invoking the attributes *attitudelabel = fixed* *withatthkset = N* *refpointlabel = user*)

We noted that despite the standard recipe for filtering proton flares, the background rate as measured in 1-10 keV bands exhibited some remnant flares. This implies that at lower energies, the proton flares turn on more slowly, yet before the main flare component. We have not chosen to further force stringent data cuts in the background template files, so that the general observer has more leeway to make an additional selection of the template files to match his/her own data selection. We emphasise that in analysing the spectrum of diffuse X-rays in the field, the recovered spectral slopes steepen with more thorough flare mitigation. Careful comparison of the recipes used for GTI creation must be made. Nevertheless it is possible that the lowest level proton fluxes are spectrally variable, and no complete subtraction can be made.

Although we noted that point sources have been removed or significantly diluted, careful examination of the images derived from these event lists reveals intensity fluctuations. Over scales of arcminutes appropriate to extended sources, it is not expected to be a significant problem, and indeed *representative* of unresolved background. However if the user should try to extract spectra from regions comparable with the mirror point spread function scale, then manual inspection might be necessary to guard against a local deficit or excess of counts arising from treatment of point sources in the template files.

As noted previously there are particular defects to be expected in the lowest energy spectral ranges. Furthermore, at the time of writing, the calibration of the EPIC soft X-ray spectral response awaits completion. The transmission of filters at energies ≤ 250 eV is difficult to measure, the CCDs' calibration at the ground synchrotron facility was not performed at energies ≤ 150 eV and the detailed redistribution of signal from photons of energies ~ 1 keV into partially collected events in the softest band was also not determined completely in ground measurements. For the time being the extension of spectral anal-

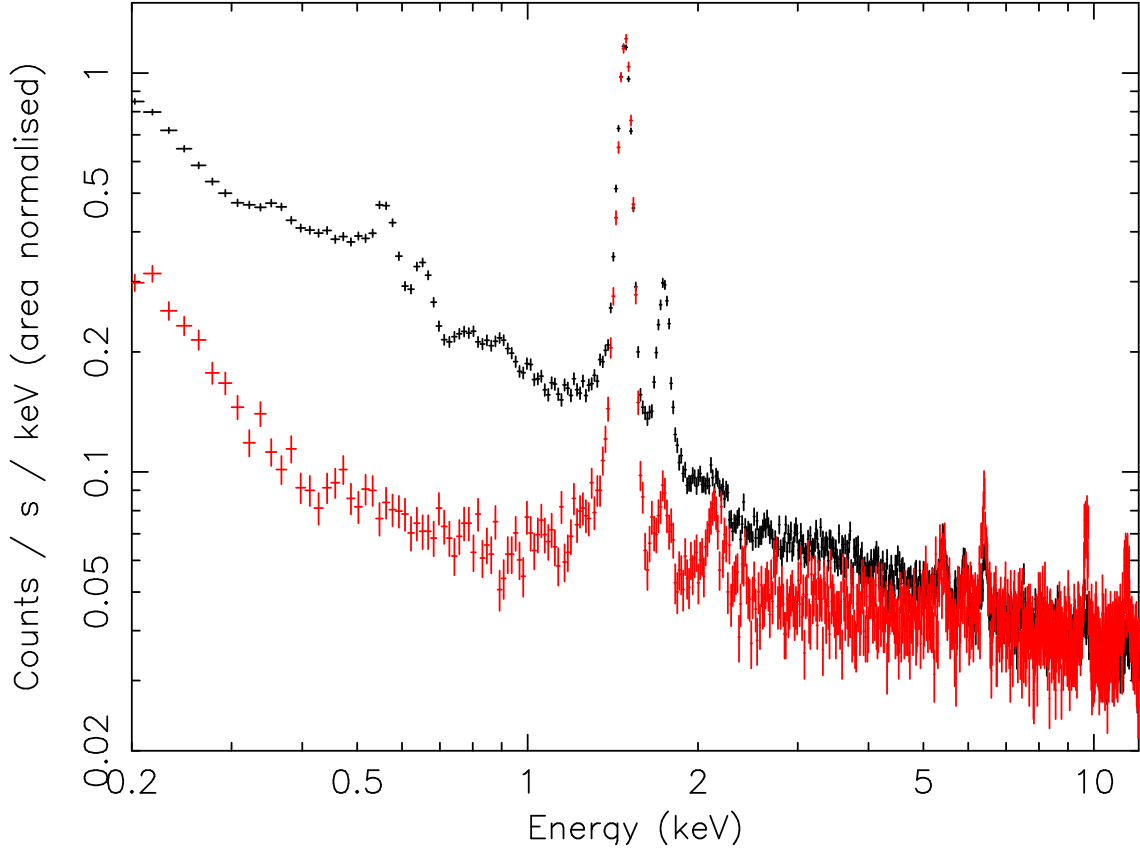


Figure 1. Comparison of internal (red) and total (including cosmic diffuse) background spectra in MOS cameras.

ysis to *any* data below 250eV should be treated with caution.

For the highest fidelity determination of background appropriate to the observer’s own data the compensation for galactic soft X-ray component, changing cosmic ray rates and different filters must be made. It is intended to provide tools within the XMM-Newton SAS environment to achieve this, but most steps should be achievable manually.

- Following suitable flare screening, define a background region (B) and extract the observed spectrum (C_{back}) from the observer’s data set. From an identical region in the template file the observed spectrum (T_{back}) should provide a measure of variability of CR component by checking count rates for $E \geq 5\text{keV}$ and/or the fluorescent emission line normalisations.
- To estimate a better internal background spectrum for the observer’s data set (C_{inst}), determine a predicted cosmic background spectrum for the observer’s region based on ROSAT ASS maps, hydrogen column etc.. An experimental tool is available at HEASARC web site. Create response matrices for the background region (here is where you can introduce the effect of different filters). Fold this cosmic spectrum through the response matrices to obtain a *predicted* cosmic compo-

nent for the background region, (C_{cos}). $C_{inst} = C_{back} - C_{cos}$

- A similar approach with the template files showed that with a weighted average N_H of $1.7 \cdot 10^{20}$ leads to a R_{45} PSPC count rate of 1.3s^{-1} in 144arcmin^2 and a 0.47-1.21 flux of $1.67 \cdot 10^{-11} \text{ ergs cm}^{-2} \text{ s}^{-1}$ for a 0.2keV R-S spectrum. This could likewise be used to make an estimate of the internal background of the template file region in order to better estimate the scaling factor (K) for CR component. $T_{inst} = T_{back} - T_{cos}$ and $K \sim C_{inst}/T_{inst}$
- Repeating the same exercise for the source region in both template and observed data sets could lead to a *predicted* background data spectrum comprising the scaled internal component, and the predicted galactic component with the appropriate filter responses.

REFERENCES

- Freyberg, M. et al 2002 in *New Visions of the X-Ray Universe* this volume
 Hasinger, G., Altieri, B., Arnaud, M. et al., 2001, A&A 365, L45
 Hopkinson, G.R. , 1992, IEEE Trans Nucl Sci 39, 2018
 Mewe, R., Gronenschild, E.H.B.M. and vd Oord, G.H.J., 1985, A&AS 62, 197